On Methods of Establishing Design Diagrams for Structural Intergrity of Slender Complex Types of Breakwater Armour Units

Burcharth, Hans F.

Published in:
Proceedings of the 2nd International Symposium on Wave Research and Coastal Engineering

Publication date:
1988

Document Version
Publisher's PDF, also known as Version of record

Citation for published version (APA):
Burcharth, H. F. (1988). On Methods of Establishing Design Diagrams for Structural Intergrity of Slender Complex Types of Breakwater Armour Units. In *Proceedings of the 2nd International Symposium on Wave Research and Coastal Engineering: Hannover, Leibnizhaus, Germany, 12-14 October 1988* (pp. 228-257)

2nd International Symposium on

Wave Research and Coastal Engineering

Oct. 12 – 14, 1988 · Hannover, Leibnizhaus

PROCEEDINGS

ON METHODS OF ESTABLISHING DESIGN DIAGRAMS FOR STRUCTURAL INTEGRITY OF SLENDER COMPLEX TYPES OF BREAKWATER ARMOUR UNITS

H.F. Burcharth
Prof. of Marine Civil Engineering, Aalborg University,
Denmark

On methods of establishing design diagrams for structural integrity of slender complex types of breakwater armour units

by

H.F. Burcharth[1]

1. Introduction

Many of the recent dramatic failures of a number of large rubble mound breakwaters armoured with Dolosse and Tetrapods were caused by breakage of the concrete armour units. Breakage took place before the hydraulic stability of intact units in the armour layers expired. Thus there was not a balance between the strength (structural integrity) of the units and the hydraulic stability (resistance to displacements) of the armour layer. Although the relative strength of the units decreases with increasing size (Burcharth 1980) the shape of the units was kept constant and not related to the size of the units and the size was not increased beyond the demand dictated by the hydraulic stability.

While the hydraulic stability can be roughly estimated by formulae and further evaluated in conventional hydraulic model tests, it is much more complicated to assess the structural integrity of the armour units.

The first methods for the estimation of the structural integrity of the slender type of armour units appeared few years ago. A method based on similarity consideration and full scale impact tests was developed for units mainly exposed to impact loads (Burcharth 1981). Instrumented small scale model armour units to measure bending movements in a cross section of the units and the accelerations (impact speed) were first used by DHL in 1980. Recent developments were presented by Scott et al. 1986. Correct scaling of the most important material properties of concrete in small scale hydraulic model tests was first presented by NRC (Timco 1981). Work based on direct strain-gauge measurement of stresses on large concrete model armour units was presented by Nishigori et al. in 1986.

So far, none of the mentioned methods have produced general applicable tools for the design of armour layers. This is mainly because the first mentioned method is related only to impact dominated units and the other methods have been used only for checking specific designs and not yet for the development or support of general design methods.

[1]Prof. of Marine Civil Engineering, Aalborg University, Denmark

Consequently there is a need for an approach by which more general information and guidelines for the design of slender armour units can be developed.

This paper deals with a general method for the development of design tools for slender type of armour units.

The first part of the paper presents a general explanation of the method. It is planned to present a second part showing an application of the method based on the results obtained from the extensive prototype research program with 42 t Dolosse at Crescent City performed by the U.S. Army Corps of Engineers WES Vicksburg (Howell 1986).

The reason for and the objective of this early presentation of the method is that, if accepted by other researchers, it might be a frame for a uniform presentation of results. Without a uniformity it will take much longer before the oncoming data on structural integrity can be made useful through contributions to the future data bank which will be needed as a design tool.

2. Overall procedure for the production of design diagrams

In principle we want a procedure for the estimation of the armour unit stresses in a specific structure as function of the sea state, i.e. we want to know the transfer functions which expresses the relationship between the stresses and the sea state, Fig. 1.

Fig. 1. Principle of transfer function analysis.

Due to the stochastic nature of the wave loads, the complex shape of the armour units and their random placement and orientation and consequently random structural support we are dealing with a problem which cannot be dealt with on a deterministic basis, but must be handled as a probabilistic problem.

The stochastic nature of the problem and the variety of the structural geometry and sea states, make it necessary to investigate a very large number of situations. This can be performed at reasonable costs only by small scale experiments with instrumented armour units, because no theory is available for quantative calculations and large scale or prototype experiments are very expensive. However, all known types of small scale model experiments produce insufficient information about the armour unit stress distribution and involve scale effects of various kinds. For this reason the principal procedure must imply a checking and calibration of the behaviours of the small scale models against recorded prototype situations where no hydraulic and structural scale effects are present.

Thus the logic procedure will be as depicted in Fig. 2.

1. Prototype investigations of stresses in concrete armour units.
2. Small scale laboratory experiments of the investigated prototype breakwater covering the recorded prototype sea state situations.
3. Comparison of prototype and small scale results and consequent calibration of the small laboratory experiment method.
4. Performance of a large number of small scale experiments comprising characteristic types of breakwaters for establishment of general design diagrams for stress response in armour units taking into account fatigue and other possible significant long term effects.

Fig. 2. Overall procedure for the establishment of design diagrams for structural integrity of armour units.

In the design process both diagrams or formulas for the hydraulic stability as well as diagrams for the structural integrity must of course be used together.

The various types of loads on armour units are listed in Fig. 3. In the following we shall consider only the static and the dynamic loads.

TYPES OF LOADS		ORIGIN OF LOADS	
STATIC		Weight of units Prestressing due to: Settlement of underlayers Wedge effect and arching due to movements under dynamic loads	
DYNAMIC	Impact	Rocking/rolling of units Missiles of broken units Placing during construction	impacting solid bodies
	Pulsating	Gradually varying wave forces including slamming Earthquake	
ABRASION		Suspended material	
THERMAL		Stresses due to temperature differences during hardening process Freeze-thaw	
CHEMICAL		Corrosion of reinforcement Sulfate reactions etc.	

Fig. 3. Type and origin of armour unit loads (Burcharth 1981).

The large number of involved parameters characterizing the sea state, the structural geometry and material, the stresses in the armour units as well as the necessarily large number of data sampled during the tests make parameter and data reduction an important question. In this respect the problem is to reduce the number of parameters in such a way that practical engineering response diagrams are established without losing significant impact from any single parameter.

Another problem is the convertion of the small scale experiment stresses to prototype stresses. This problem stems from the fact that generally three types of loads and corresponding stresses can occur, Fig. 4.

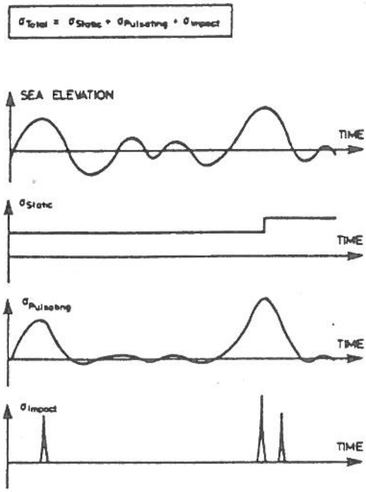

Fig. 4. Types of stresses in armour units (Burcharth 1984).

However, these stresses do not scale the same way, as is indicated in Fig. 5.

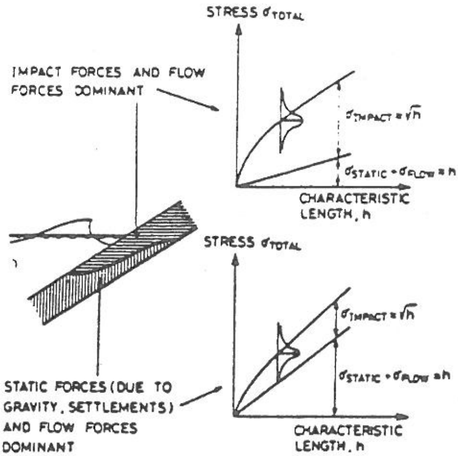

Fig. 5. Qualitative representation of stresses in complex armour units as function of the size (length) of the units (Burcharth 1986).

Generally in complex types of armour units the stress level due to flow forces (drag and slamming) and static (gravity, including effects of settlements) forces increases linearly with the characteristic length (e.g. the height of the armour unit) while the stress level due to impacting units (dynamic stress waves) increases with the square root of the characteristic length. The relative importance of these stresses depends on the geometry of the units and their position on the slope. For this reason a correct conversion to another length scale can be performed only if also the ratio between the two types of stresses is known. Consequently the measured strain/stress signal must be analysed accordingly. This is possible because the duration of an impact stress pulse (from impacting solid bodies) is in the order of milli-seconds (in prototype), several order of magnitudes less than the duration of flow forces cycles including slamming. In principle a strain/stress signal must be analysed as shown in Fig. 6.

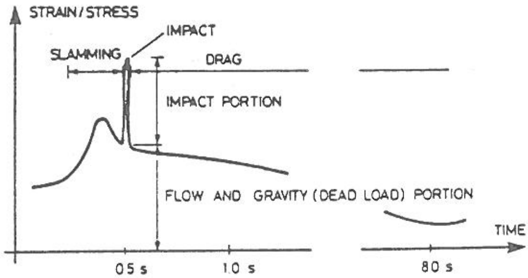

Fig. 6. Illustration of prototype strain signal comprising all types of strains/stresses.

When converting to other scales it must of course be checked, if a recorded strain/stress maximum which is not the largest within a wave cycle (e.g. the one at 0.4 sec in Fig. 6) represents the largest strain/stress.

One of the most difficult problems to overcome is the fact that impact stress (caused by impacting armour units) cannot be correctly reproduced in small scale models due to material characteristics different from prototype concrete and ultra short pulse durations. For this reason one has to study the nature and magnitude of the impact stresses (probability density functions) in prototype experiments or in large scale models with concrete armour units of $50 - 100$ kg and then analytically add statistically correct contributions from impact to the stresses measured in the small scale armour units.

Another problem is the correct reproduction of the prototype armour surface roughness in the model. A non-correct model armour surface roughness might cause a significant scale effect.

3. Data reduction

3.1 Structural parameters:

The transfer functions, as defined in Fig. 1, are related to the geometry and the material characteristics of the breakwater elements, i.e. they depend on a large number of parameters. Since we dot not have general formulae or theories which give the relationships, we must study the problem on an empirical basis by performing experiments. Because it is not possible to overcome a systematical variation of all parameters we can, first of all, restrict ourselves to simple types of armour layer geometries by leaving out multislopes and concrete cappings. Secondly we can retain only the most important parameters and finally try to group them in dimensionless parameters.

If we are dealing only with unreinforced slender types of armour units made of normal concrete and placed at random in a "normal" two layer system, we must as a minimum include the parameters indicated in Fig. 7.

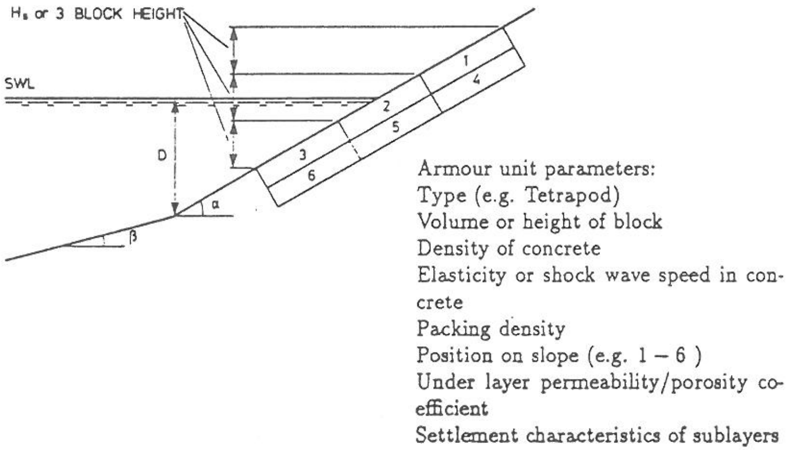

Fig. 7. Proposal for structural parameters.

The parameters β (fore-shore slope) and D (depth at toe) are more logically included/implemented in the sea state parameters and thus being excluded from the structural parameters.

As an alternative to the use of the significant wave height H_s as a measure for the extension of the six armour unit position areas, one could use a multiplum of the characteristic height h of the armour unit, e.g. $3 \cdot h$.

Instead of keeping track of the unit position on the slope by dividing the slope into six areas (which is proposed to overcome the problem with upscaling of the stresses, cf. Fig. 5) one could for simplicity just use one area covering the same total portion of the slope. This will of course reduce the number of transfer functions to 1/6 , but will also result in a larger scatter in the transfer function and somewhat reduced possibilities for a rational transformation of stresses into other length scales.

In principle there will be a transfer function for each combination of the above given structural parameters if we cannot combine them in meaningful groups or delete those of minor importance. This is a subject for further research.

3.2 Sea state (environmental) parameters:

It is assumed that the wave action is head on to the structure.

The waves can be described either by a deterministic wave by wave analysis based on zero-crossings in the time domain, Fig. 8, or by the variance (power) spectrum in the frequency domain, Fig. 9.

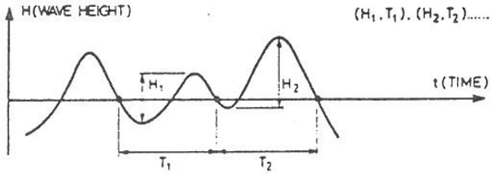

Fig. 8. Zero-crossing definition of waves.

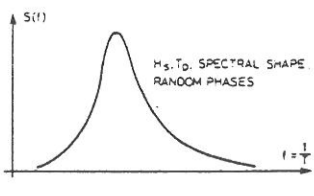

Fig. 9. Waves defined by power spectrum.

Using the zero-crossing definition implies a "wave by wave" response analysis which is meaningful only if the wave record is from a position so close to the breakwater (few wave lengths) that the succession and the character of the waves are not changed. If the distance is app. $1 - 1.5$ wave length then the effect of the fore-shore characteristics on the waves are to some extend automatically implemented. It should be noted that wave reflection might bias the wave trains, but this effect will in most cases be insignificant compared with the expected scatter in the analysis. It is necessary, also, to have simultaneous recordings of the waves and the armour unit response to be able to optimize the correlation the two signals (by shifting the wave signal in time corresponding to the average wave celerity times the distance from the wave gauge to the armour slope). Because we are dealing with wave loads the "down" crossing definition of waves (as shown in Fig. 7) should be used, because this produces oncoming wave heights as seen from the breakwater.

It might be useful to combine H and T in a surf-similarity parameter (Irribarren number or breaker parameter) since this parameter determines the type of wave breaking on the slope and thereby also the type of impact. For a wave by wave analysis this parameter would be $\zeta = T\left(\frac{2\pi}{gH}\right)^{0.5}\tan\alpha$. It should be noted that although the slope α is included in ζ , it cannot be omitted as one of the structural parameters, because the armour unit stress response will depend on a α-term, which cannot from a theoretical point of view be implemented or combined in a ζ-term.

By performing a wave by wave analysis it is in fact assumed that the armour layer response is uniquely related to each separate wave defined solely by its H and T. Consequently the wave succession/wave grouping (the effect of the preceding wave) is not registered in the input, but it will of course be inherent in the output, cf. Fig. 1. This result in more scatter in the transfer function simply due to the fact that a specific wave defined by its H and T will impose different stresses in the armour units dependent on its position in the wave train.

If – in stead of the wave by wave analysis in the time domain – we perform the analysis in the frequency domain, the wave power spectrum must be taken as the input, Fig. 9. It is assumed that we are dealing with random phases of component waves, i.e. the groupiness is determined by (inherent in) the spectral shape. The output of the analysis should be a stress transfer function hopefully generally applicable to any realistic wave spectrum. If such a goal can be achieved is not certain due to the non-linearities in the system. However, a method of coping with non-linearities will be discussed in Appendix B.

If we limit the general analysis to single peak spectra (omitting double peak spectra usually caused by combined swell and storm waves) it might be sufficient to characterize the spectrum solely by its characteristic values of heights and periods, i.e. H_s and T_p (or T_z) and subsequently relate the stress-response values to these parameters leaving out specification of the spectral shape. This proposal is supported by rock stability tests by Van der Meer et al. (1986) and run-up tests on armoured slopes by Allsop et al. (1985) where no significant influence of the type of spectra was found (Jonswap/Pierson-Moskowitz). Van der Meer used T_z as characteristic wave period whereas Allsop et al. used T_p.

H_s and T_p might be combined in the breaker parameter

$$\zeta = T_p\left(\frac{2\pi}{g\,H_s}\right)^{0.5}\tan\alpha$$

The spectrum must represent the sea state close to the structure. If for shallow water structures, only a deep water spectrum is available then a transformation of the spectrum to a shallow water position in front of the structure must be performed.

3.3 Armour unit stress parameters:

Since for unreinforced concrete armour units the exceedence of the tensile strength at any point of the body is a reasonable failure criterion, it seems reasonable to convert the recorded strains to a single parameter being the maximum principal tensile stress, σ_1.

In the case of wave by wave response analysis the parameter value of the stress should be "the maximum peak value" within each wave period.

In the case of a response analysis in the frequency domain we must obtain a stress power spectrum based on a continuous signal of the variation of σ_1 with time.

The basis for the calculation of σ_1 will be strain measurements in instrumented sections of the armour units.

Other sections than the instrumented one(s) might experience larger stresses. For such sections estimates on σ_1 might be produced by means of finite element analysis simulations.

As explained in section 2 various types of forces contribute to the stress σ_1. Unfortunately stresses generated by impact forces scale differently from gravity and flow force generated stresses. Consequently the component stresses (or forces) should be scaled correctly before being added to form the total stresses.

Because the maximum stresses generated by the various types of forces do not occur in the same point within a cross section of the armour unit one has in principle to determine the component stresses over the entire cross section in question, then add them and finally extract the maximum value. Such a procedure involves a lot of computation. An easier approach would be to determine the cross section force components (bending moments M_y, M_z, torque, T, shear forces V_y, V_z and axial force, N_x) for each type of loads, convert them to prototype scale, add them and then calculate the maximum principle tensile stress, σ_1. Appendix A explains as an example the calculation of σ_1 for an instrumented cross section of a Dolos.

The ultra short duration of impact loads makes it necessary not only to sample data with a very high frequency but also to perform a large number of stress calculations densily spaced in the time to ensure identification of the stress peak value. Identification of the impact generated peaks in the strain gauge signals might be very difficult when dealing with small prototype armour units and almost impossible in case of small scale model armour units. The latter might in any case be useless due to non correct material characteristics for such units.

Also from a computational point of view it is a great complication that impact induced stresses have to be separated from the total stresses, cf. Fig. 6. In the case of a response analyses in the frequency domain, i.e. the transfer function is obtained from a continuous wave amplitude signal and a continuous principal stress signal, it is practically impossible to separate the impact induced stresses.

Hopefully, the wave by wave response analysis will show that even for large armour units it will be reasonable to separate the armour response in the following two categories, cf. Fig. 5.

1. Units not moving and not being exposed to significant impacts from other units.

   Such units are predominantly situated in the armour under-layer. The linear scaling of stress with the length scale can be applied and will be on the safe side in case of some impact generated stress contributions.

2. Units rocking and being displaced.

   Such units are predominantly sitting in the top layer in a zone around mean water level. Impact generated stresses will be a dominant part of the total stresses and can be treated in accordance with the non-linear scaling law. Because this scaling law is on the unsafe side if flow and gravity generated stresses of any significance are present an estimated correction might be performed.

4. Presentation of stress transfer functions and design procedure

The transfer function analyses and proposals for the presentation of the stress transfer functions are schematized in Fig. 10.

For each type of armour unit its mass and packing density and position on the slope as well as under layer permeability and slope geometry there will be one transfer function (h is characteristic length of armour unit) cf. Fig. 7.

Deterministic wave by wave analysis (time domain)

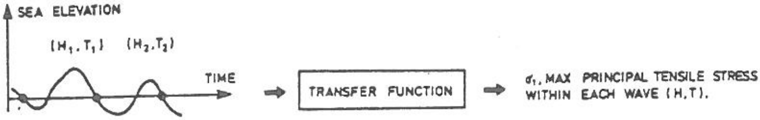

Stochastic spectral analysis (frequency domain)

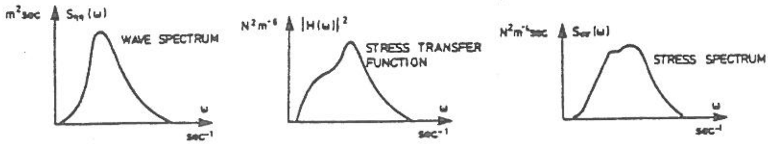

Proposal for presentation of transfer functions

If no significant impact stresses are present there will be a linear relationship between stress and characteristic length. For such cases the transfer functions might be presented as shown below provided we are dealing with single peak wave spectra.

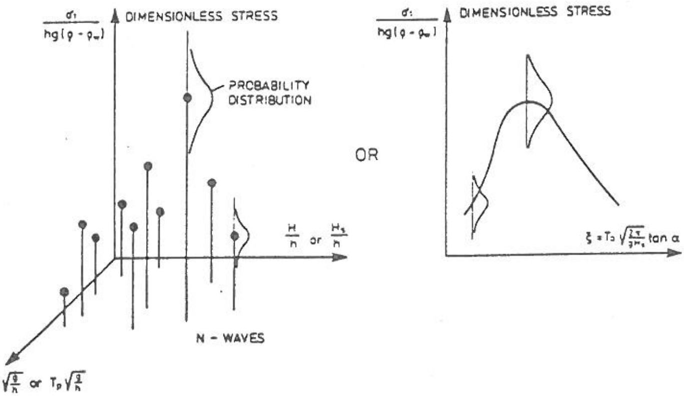

If significant impact stresses are present the transfer function diagrams cannot be made dimensionless as shown above. For such cases special diagrams showing the relationship between σ_1, H and T for characteristic ratios of impact stress to total stress must be produced.

Fig. 10. Outline of transfer function analysis.

The design procedure is outlined in Fig. 11.

1. Scale σ_1 from transfer function diagrams to obtain prototype scale stress, $\sigma_1^{prototype}$. (Take into account ratio of impact stresses to total stresses)
2. Determine the max allowable prototype stress, $\sigma_1^{critical}$ on the basis of the concrete tensile strength and the fatigue during the structural lifetime.
3. If $\sigma_1^{prototype} > \sigma_1^{critical}$ change size or type of armour unit until the prototype stress do not exceed the critical stress.
4. Check the hydraulic behaviour of the armour layer.

Fig. 11. Procedure for use of stress transfer functions in the design procedure.

The fatigue effect can be very significant as shown in Fig. 12.

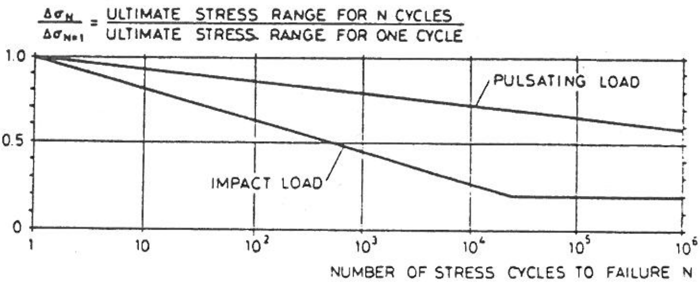

Fig. 12. Fatigue in complex type armour unit made of conventional unreinforced concrete. Uniaxial and flexural stress (Burcharth, 1984).

The graphs are based mainly on studies of fatigue in concrete armour units and are regarded accurate enough for practical design of armour layers made of conventional unreinforced concrete blocks. It should be noted that the ultimate *impact load* strength for one cycle is in the order of 1.4 and 1.5 times the ultimate *pulsating load* strength in the case of uniaxial tension and compression respectively. For flexural stresses a factor of app. 1.4 should be used.

The ultimate pulsating load strength properties for one cycle can be taken equal to the static ones.

The fatigue life is usually evaluated according to the *Palmgren-Minor accumulated damage theory* on the basis of a propriate Wöhler diagram, e.g. Fig. 12.

The Palmgren-Minor rule expressing the cumulative damage ration, D reads

$$D = \sum_{i+1}^{K} \frac{n_i}{N_i} \leq 1$$

where η_i is the number of cycles within the stress range interval i, N_i is the number of cycles to failure at the same stress range derived from the Wöhler diagram and K is the total number of stress range intervals. This implies that the number of stress cycles and the corresponding stress range throughout the lifetime of the structure, i.e. η, N and K must be estimated. This again means that the *load history* and the *relationship between the load and the stresses* must be established. The latter is given by the stress transfer functions.

5. References

Allsop, N.W.H., Hawkes, P.I., Jackson, F.A., Franco, L. (1985): Wave run-up on steep slopes - Model tests under random waves. Hydraulics Research Wallingford, Report No. SR2, August 1985.

Burcharth, H.F. (1980): Full-scale dynamic testing of Dolosse to destruction. Coastal Engineering 4, pp 229-251, 1981.

Burcharth, H.F. (1984): Fatigue in breakwater concrete armour units. Proc. 19th Int. Conf. on Coastal Engineering, Houston, Texas, 1984.

Burcharth, H.F. (1986): The influence of waist thickness of Dolosse on the hydraulic stability of Dolosse armour. Proc. 20th Int. Conf. on Coastal Emgineering, Taipei, Taiwan, 1986.

DHL Hydro Delft No. 56, March 1980, Delft Hydraulics Laboratory. Holland.

Howell. G.L. (1986): A system for measurement of the structural response of Dolos armour units in the prototype. The Dock & Harbour Authority, Vol. 67, No. 779, May 1986.

Scott, R.D., Turcke, D.J., Baird, W.F. (1986): A unique instrumentation scheme for measuring loads in model Dolos units. Proc. 20th Int. Conf. on Coastal Engineering, Taipei, Taiwan, 1986.

Timco, G.W. (1981): The development, properties and production of strength-reduced model armour units. Lab. Tech. Report, Nov. 1981. Hydraulics Lab. Ottawa, NRC, Canada.

Van der Meer, J.W., Pilarczyk, K.W. (1986): Dynamic stability of rock slopes and gravel beaches. Proc. 20th Int. Conf. on Coastal Engineering Conference, Taipei, Taiwan, 1986.

Appendix A

STRESS ANALYSIS illustrated by an analysis related to model Dolos armour units

Component forces
The following types of forces contribute to the stresses in an armour unit in a pack exposed to waves:

1. Gravity forces; Compaction forces (mainly due to settlements, gravity and flow forces)
2. Flow forces
3. Impact forces (impacts between moving concrete blocks)

Stresses created by 1 and 2 have a linear dependency on the length scale (e.g. the height of the Dolos) while stresses created by 3 have a non-linear dependency (proportional to the square root of the length scale). *Because the stresses scale differently the component stresses (forces) should be scaled correctly before being added to form the total stresses.*

It is believed that the easiest way is to determine the cross section force component $M_y, M_z, N_x, T, V_y, V_z$ for each type of load from whatever source is available, scale them to prototype scale and then add them. The probability of simultaneous occurrence must of course be taken into account. After this the stress situation in the sections can be determined as described in the following.

The objective of the present research project is to determine stresses created by the class 1 forces only.

Cross section force components
For each of four instrumented sections (1 - 4) of the Dolos the following quantities are calculated from recordings of the strains in a circular steel pite:

M_y and M_z, bending moments
N_x, normal force
T, torsio
V_y and V_z, shear forces.

The *local* coordinate systems shown in Fig. 1 are used.

As seen from Fig. 1 the x -coordinate is always normal to the section (parallel to the axes of the Dolos). The $x - y$-coordinate plane is parallel to the shank - fluke plane and consequently it changes at the mid shank cross section.

This local coordinate system is used for the analysis of the stresses in the instrumented cross sections.

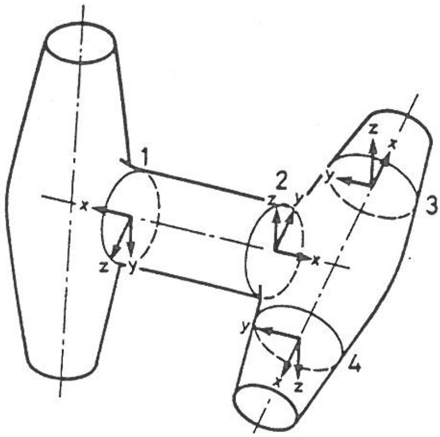

Fig. 1. Local coordinate system.

The stresses in other parts of the Dolosse might be estimated on the basis of the stresses found in the instrumented sections. However, for such an analysis the global coordinate system shown in Fig. 2 is used.

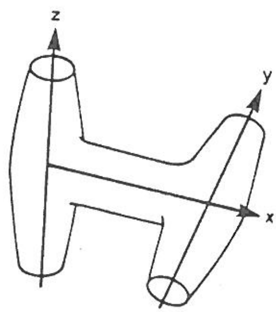

Fig. 2. Global coordinate system.

Data reduction

It should be checked if a 2-D representation of the stress field is a reasonable approximation. This can be done by comparison with a 3-D representation.

Moreover, it might be possible to leave out the stress contribution from normal and shear forces as they are expected to be of minor importance compared to bending moments and torsion. This should be checked.

The last point is relevant also because in most ongoing experiments (prototype and small scale) only bending moments and torsion are recorded.

If only bending moments and torsion are of importance then it is clear that the maximum tensile stresses are to be found at the surface of the body.

A polar coordinate system might then be more handy especially if the cross section is approximated to a circular section, Fig. 3. If the octahedal cross section is kept the di-

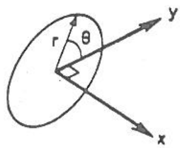

Fig. 3.

stribution of a residual stress capacity function, F, along the cross section surface should be investigated with the purpose of reducing the number of points of analysis to the eight surface corner points. However, the circular section is much easier to deal with and is a very close approximation as shown in the following.

Analysis of stresses

- The concrete is assumed linear elastic.
- Failure is defined as occuring when the tensile stress of any point reaches the tensile strenght of the unreinforced concrete.
- For the evaluation of the stress conditions in a cross section the 2-dimensional principal stress failure criterion will be used

$$f = -(\sigma_1 - S)(\sigma_2 - S) \leq 0 \qquad \text{(no failure)} \qquad (1)$$

σ_1 and σ_2 are the principal stresses, positive as tension. S is the tensile strength.

Eq (1) is to be interpreted in such a way that the failure area is defined as depicted in Fig. 4. (σ_1 and σ_2 cannot simultaneously be larger than S without causing failure. Failure will occur if either $\sigma_1 - S \geq 0$ or/and $\sigma_2 - S \geq 0$).

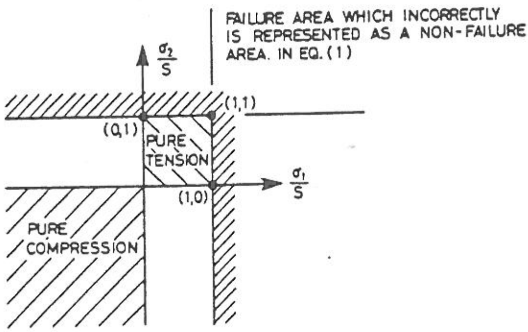

Fig. 4. 2-dimensional principal stress failure criterion.

Although the stress conditions in reality are 3-dimensional it is a resonable approcimation to use a 2-dimensional stress failure criterion because the most critical stress conditions are known to occur at the surfaces of the body.

Thus only stress conditions at points on the surface are considered in the analysis.

A local coordination system as shown in Fig. 5 is used. The x-coordinate is normal to section in question and the α - coordinate is parallel to the surface at the point of consideration. While the x - coordinate orientation is fixed relative to the cross section of the Dolos the α - coordinate changes orientation dependent on the position of the point of analysis, P, given by the angle, θ.

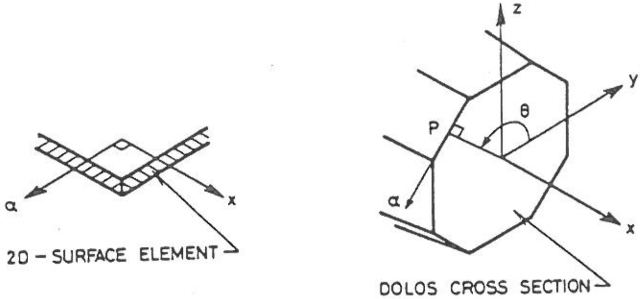

Fig. 5. Coordinate system.

Eq. (1) can be expanded to

$$f = -(\sigma_1\sigma_2 - S(\sigma_1 + \sigma_2) + S^2)$$

$$= -(\sigma_{xx}\sigma_{\alpha\alpha} - \sigma_{x\alpha}^2 - S(\sigma_{xx} + \sigma_{\alpha\alpha}) + S^2) \leq 0 \quad (2)$$

or

$$F \equiv \frac{f}{S^2} = \frac{\sigma_{x\alpha}^2}{S^2} - \frac{\sigma_{xx}\sigma_{\alpha\alpha}}{S^2} + \frac{\sigma_{xx} + \sigma_{\alpha\alpha}}{S} - 1 \leq 0 \quad (3)$$

F may be regarded a dimensionless measure of the residual stress capacity in the specific point.
Note the non-linear dependency of F on the stresses.

The quantity F is suitable for statistical treatment but only if representing the resulting stress conditions caused by all types of simultaneously present forces as mentioned earlier. This implies that contributions to $\sigma_{x\alpha}$, σ_{xx} and $\sigma_{\alpha\alpha}$ from each of the earlier mentioned types of forces (gravity/compaction, flow and impact forces) must be determined before a meaningful value of F can be found.

Due to the earlier mentioned different scaling with block size of the stresses created by the various types of loads one has to scale to prototype the component stresses $\sigma_{x\alpha}$, σ_{xx} and $\sigma_{\alpha\alpha}$ before F can be calculated.

As discussed in the last part of the section it is probably easier to operate with the maximum principal tensile stress instead of the failure function, F.

Calculation of the residual stress capacity function
The two-dimensionless residual stress capacity function (failure function) F given by eq. (3) can be found from the force component.

F is related exclusive to the stress (strain) condition in a specific point at the surface of the body.

Fig. 6 shows the cross section and the local coordinate system.

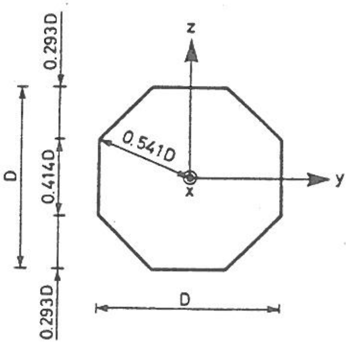

Fig. 6. Cross section with local coordinate system.

The force component M_y, M_z, N_x, T, V_y and V_z related to the local coordinate system, Fig. 5, are determined from recordings of strains in an instrumented section of a steel pipe inserted in the Dolos as shown in principle in Fig. 7.

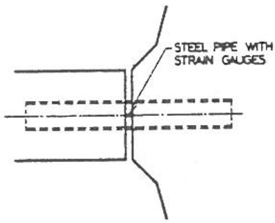

Fig. 7. Principle of instrumented sections.

The transformation of the above mentioned force component into the stress components σ_{xx}, σ_{yy}, σ_{xy} as given by eq. (3) and the coordinate system Fig. 3 is performed as follows:

For simplicity we shall use a circular cross section as a close approximation to the octahedal cross section. Because the maximum tensile stresses are supposed to be at the surface of the Dolos the choise of diameter of the circular section must be based on minimum deviation of the stresses at the surface.

It can be shown that if the normal forces or the bending moments are the only contributors to the stresses at the surface then the diameter d of the „equivalent" circular section should be d = 1.027 D or d = 1.023 D respectively. Because most likely the bending moments will be the main contributor to the tensile stresses a diameter d = 1.024 D is chosen for the equivalent cross section, Fig. 8.

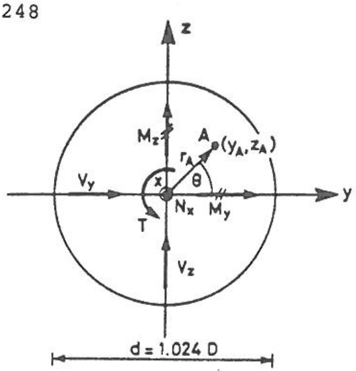

Areas of section $F = \pi(\frac{d}{2})^2$

Modulus of section $I_y = I_z = I = \frac{\pi}{64} d^4$

Fig. 8. Equivalent circular cross section.

For a circular cross section with diameter, d, one can derive the following analytical expressions for the stress components

normal stress component in direction x

$$\sigma_{xx} = \frac{N_x}{F} + \frac{M_y}{I_y} z_A - \frac{M_z}{I_z} y_A \qquad (4)$$

shear stress component in direction y

$$\sigma_{xy} = \frac{3+2\nu}{8(1+\nu)} \frac{V_y}{I_z} \left[(\frac{d}{2})^2 - y_A^2 - \frac{1-2\nu}{3+2\nu} z_A^2 \right] - \frac{1+2\nu}{4(1+\nu)} \frac{V_z}{I_y} y_A z_A - \frac{T}{I_x} z_A \qquad (5)$$

shear stress component in direction z

$$\sigma_{xz} = \frac{3+2\nu}{8(1+\nu)} \frac{V_z}{I_y} \left[(\frac{d}{2})^2 - z_A^2 - \frac{1-2\nu}{3+2\nu} y_A^2 \right] - \frac{1+2\nu}{4(1+\nu)} \frac{V_y}{I_z} y_A z_A + \frac{T}{I_x} y_A \qquad (6)$$

ν is Poisson's ratio.

The formulae (5) and (6) fulfil the requirement that no stress component at right angle to the surface exists when only the above mentioned force components are present, i. e. no contact loads acting on the surface in the point of analysis.

At the surface eqs (4), (5), and (6) reduces to

$$\sigma_{xx} = \frac{N_x}{F} + (\frac{M_y}{I}\sin\theta - \frac{M_z}{I}\cos\theta)\frac{d}{2} \tag{7}$$

$$\sigma_{xy} = \frac{1+2\nu}{4(1+\nu)I}(\frac{d}{2})^2\left[V_y\sin^2\theta - V_z\sin\theta\cos\theta\right] - \frac{T}{I_x}\frac{d}{2}\sin\theta \tag{8}$$

$$\sigma_{xz} = \frac{1+2\nu}{4(1+\nu)I}(\frac{d}{2})^2\left[V_z\cos^2\theta - V_y\sin\theta\cos\theta\right] + \frac{T}{I_x}\frac{d}{2}\cos\theta \tag{9}$$

$I_x = 2I$ for the circular cross section.

With reference to the surface coordinate system given in Fig. 5 it is seen that the shear stress component $\sigma_{x\alpha}$ is given as

$$\sigma_{x\alpha} = \sigma_{xz}\cos\theta - \sigma_{xy}\sin\theta \tag{10}$$

cf. Fig. 9.

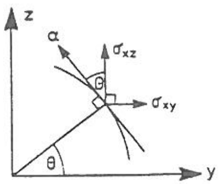

Fig. 9.

$$\sigma_{x\alpha} = \frac{1+2\nu}{4(1+\nu)I}(\frac{d}{2})^2(V_z\cos\theta - V_y\sin\theta) + \frac{T}{I_x}\frac{d}{2} \tag{11}$$

Note that the stress component $\sigma_{\alpha\alpha}$ given in eq. (2) is zero if only the cross section force components given by N_x, M_y, M_z, V_y, V_z and T are present. This is actually the case because the components are found solely from strain measurement in a section of the inserted steel pipe where no surface loads are present.

Transforming these force components to equivalent stresses at the Dolos concrete surface gives of course no possibility of determining a stress component $\sigma_{\alpha\alpha}$. Such a component of some magnitude might exist if significant contact loads from neighbour Dolosse are present at or near the section where the stresses are determined. However, because the most critical sections (i. e. sections where maximum tensile stresses are expected to occur) are thought to be near the trunk-shank corners where contact points with other blocks are less likely to occur it is assumed that $\sigma_{\alpha\alpha}$ can be ignored. This of course should be verified in some way – most probably by FEM simulations.

$\sigma_{\alpha\alpha}$ could of course be found by means of strain gauge rosettes placed directly on the Dolos concrete surface. This method was actually tried in the present case but did not work due to too small strains generated in the 200 kg Dolosse. Much larger Dolosse are needed for this method.

If $\sigma_{\alpha\alpha}$ is ignored then the residual stress capacity criterion given by eq. (3) reduces to

$$F = \frac{\sigma_{x\alpha}^2}{S^2} + \frac{\sigma_{xx}}{S} - 1 < 0 \tag{12}$$

For a Dolosse placed in a certain position in a specifik pack of blocks the stress components in eq. (12) are functions of the position of the considered cross section and the angle θ.

Due to the symmetry of a Dolos the probability density function (pdf) $F(\theta)$ will be identical for sections 1 and 2 and for sections 3 and 4 when the local coordinate systems are defined as depicted in Fig. 1 and the Dolosse are placed at random. Moreover, for sections 1 and 2 we have

$$\text{pdf } F(\theta) = \text{pdf } F(180° - \theta) \quad \text{and pdf} F(180° + \theta) = \text{pdf}(-\theta) \tag{13}$$

and for sections 3 and 4

$$\text{pdf } F(\theta) = \text{pdf } F(-\theta) \tag{14}$$

Fig. 10 shows in principle for one section the outcome of a single test.

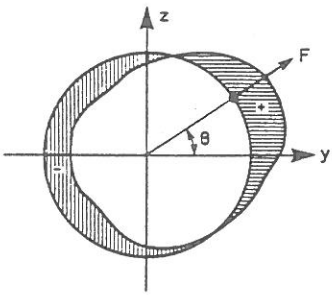

Fig. 10. Illustration of outcome of a single test.

If the tensile strength of the concrete is S then we can define the following critical quantities that produce cracking in the surface due to bending moments, torque, shear forces and normal forces respectively

$$
\begin{aligned}
M_{cr} &= S\frac{2I}{d} \\
T_{cr} &= S\frac{I_x}{\frac{d}{2}} = S\frac{4I}{d} \\
V_{cr} &= S\frac{4I}{d^2} \\
N_{cr} &= S\cdot F
\end{aligned}
\qquad (15)
$$

Substituting eqs. (15) into eq. (12) using eqs. (7) and (11) gives the following expression for the dimensionless residual stress capacity function

$$
F = \frac{M_y\sin\theta - M_z\cos\theta}{M_{cr}} + \left(\frac{T}{T_{cr}}\right)^2 + \left(\frac{\frac{1+2\nu}{4(1+\nu)}\,(V_z\cos\theta - V_y\sin\theta)}{V_{cr}}\right)^2
$$

$$
+ \frac{2T\,\frac{1+2\nu}{4(1+\nu)}\,(V_z\cos\theta - V_y\sin\theta)}{T_{cr}\cdot V_{cr}} + \frac{N}{N_{cr}} - 1 \leq 0 \qquad (16)
$$

The values of M_{cr} and T_{cr} should be based on linear stress distributions, i.e. for a circular cross section with diameter, d

$$M_{cr} \simeq 0.10d^3\cdot S$$

$$T_{cr} \simeq 0.20d^3\cdot S$$

It is regarded un the unsafe side to assume a non-linear stress distribution caused by simultaneously yielding over the entire cross section. For such conditions we find $M_{cr} \simeq 0.15d^3\cdot S$.

Instead of operating with the stress component σ_{xx} and $\sigma_{x\alpha}$ or with the residual stress capacity function F, one can operate with the *max principal tensile stress*, $\sigma_1 = \sigma_{max}$. σ_1, which is a function of θ, can be found from Mohr's diagram as follows, cf. Fig. 11.

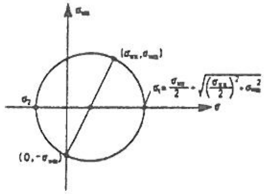

$$\sigma_1 = \frac{\sigma_{xx}}{2} + \sqrt{\left(\frac{\sigma_{xx}}{2}\right)^2 + \sigma_{x\alpha}^2} \tag{17}$$

Fig. 11. Mohr's diagram.

The angle β between σ_1 and σ_{xx} is given by

$$tg\,2\beta = \frac{\sigma_{x\alpha}}{\frac{1}{2}\sigma_{xx}} \tag{18}$$

The angle β is in the 2-dimensional surface element plane, Fig. 12.

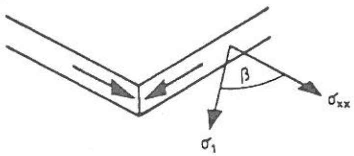

Fig. 12. Illustration of orientation of σ_1.

To arrive at correct estimates of the prob. failure it must be verified if σ_1 and σ_2 are not $> S$ simultaneously, cf. eq. (1).

Conclusion

The most convenient parameter to use is most probably $\sigma_1(\beta)$.

Acknowledgements

Valuable comments and suggestions by Dr. L. Pilegaard Hansen and Dr. A. Rathkjen, Inst. of Building Technology and Structural Engineering, University of Aalborg, are appreciated.

Appendix B

Calculation of transfer functions by means of frequency domain correlation analysis

The transfer function is found on the basis of simultaneously recorded wave amplitude signals $\eta(t)$ and force or stress signals.

Filtering of signals
The mean force (or stress) contributions, $\Delta\sigma_{static}$ caused by the static loads are removed from the force (or stress) signal to obtain only the varying part $\sigma(t)$. $\Delta\sigma_{static}$ has to be added at a later stage.

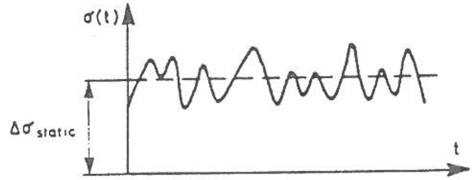

Fig. 1. The mean $\Delta\sigma_{static}$ is removed from the signal.

Because we have to treat $\eta(t)$ and $\sigma(t)$ as stationary random functions of time the lengths of the records are limited to stationary sequences. However, the signal should contain at least 100 waves and preferably more than 200 waves.

Determination of separation time for optimum correlation
In case of wave by wave analysis the effect in terms of max σ of every single wave is identified. Because wave recording takes place at some distance, ℓ from the structure, the wave signal must be shifted $\Delta t = \ell/c$ in time, to obtain the optimum time-space correlation. The wave celerity, c can be calculated in case of regular waves. However, for irregular waves a deterministic calculation of c is not possible. Instead Δt can be found from the cross correlation function, Fig. 2.

$$R_{\eta\sigma}(\tau) = E\left[\eta(t) \cdot \sigma(t+\tau)\right] \tag{1}$$

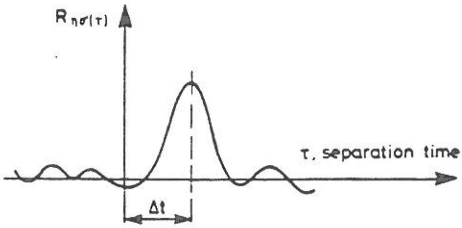

Fig. 2. Determination of time lag corresponding to optimum correlation between wave and stress signals.

Check on linearity

In general a partly non-linear relationship between the wave amplitude signal $\eta(t)$ and the stress signal $\sigma(t)$ is to be expected. This is due to the variation in time of the flooding of some units during wave action and due to the drag term inherent in the Morison flow force formula (eq 2), which for the non breaking portion of the waves will produce a non-linear relationship between $\eta(t)$ and $\sigma(t)$. This is because σ will be proportional to F, and U approximately proportional to η.

$$F = \frac{1}{2} \cdot \rho \cdot C_D \cdot U \cdot |U| \cdot A + \rho \cdot C_M \cdot \dot{U} \cdot V \qquad (2)$$

ρ is the mass density of water, U is the flow velocity, A and V are the cross section area and the volume of the body, respectively. And C_D and C_M are the drag and intertia coefficients, respectively.

For breaking waves one might estimate U to be approximately proportional to $\sqrt{\eta}$, which will produce linearity between η and σ.

The degree of linearity can be investigated by means of the coherence function

$$\gamma^2_{\eta\sigma}(\omega) = \frac{|S_{\eta\sigma}(\omega)|^2}{S_{\eta\eta}(\omega) \cdot S_{\sigma\sigma}(\omega)} \qquad (3)$$

where

$S_{\eta\eta}(\omega)$ = wave amplitude spectrum
$S_{\sigma\sigma}(\omega)$ = stress amplitude spectrum
$S_{\eta\sigma}(\omega)$ = cross-spectrum, i.e. the Fourier transform of the cross correlation function $R_{\eta\sigma}(\tau)$

The coherence function is a measure of the linear dependency between the two signals. It will be unity at frequencies were linearity exists, cf. Fig. 3.

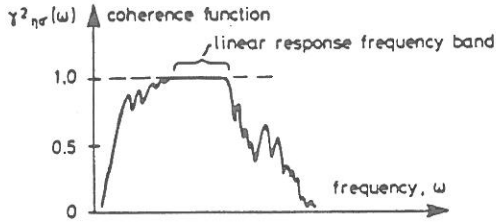

Fig. 3. Example of coherence function.

Calculation of the transfer function for a linear system
If the coherence function indicates linear dependency between $\eta(t)$ and $\sigma(t)$ on frequencies where significant stresses occur and if we assume a time invariant system then the transfer function $H(\omega)$ can be calculated in the following three ways:

$$|H(\omega)|^2 = \frac{0.5\ a_\sigma^2(\omega)}{0.5\ a_\eta^2(\omega)} = \left(\frac{a_\sigma(\omega)}{a_\eta(\omega)}\right)^2$$

or

$$|H(\omega)| = \frac{a_\sigma(\omega)}{a_\eta(\omega)} \tag{4}$$

where a stands for amplitude.

$$|H(\omega)|^2 = \frac{S_{\sigma\sigma}(\omega)}{S_{\eta\eta}(\omega)} \tag{5}$$

$$|H(\omega)| = \frac{S_{\eta\sigma}(\omega)}{S_{\eta\eta}(\omega)} \tag{6}$$

Fig. 4 illustrates the transfer function.

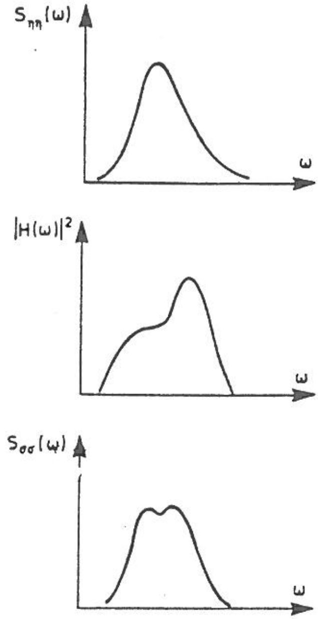

Fig. 4. Illustration of transfer function for a linear system.

When dealing with a stationary random process that are transformed by a linear time-invariant system the response $\sigma(t)$ will be Gauss-distributed if such is the input. This means that if the wave heights of the wave amplitude signal $\eta(t)$ are Rayleigh - distributed the the maximum values of the stress signal $\sigma(t)$ will also be Rayleigh - distributed. To get the total stress one must add the static part $\Delta\sigma_{static}$ which was extracted from the signal. For this purpose the joint probability density function for $\sigma(t)$ and $\Delta\sigma_{static}$ must be known.

Calculation of the transfer function for a non-linear system
If the coherence function indicates a non-linear system then the following linearization procedure might be applied.

It is assumed that the stress can be given in the form of a Morison type equation

$$\sigma = C_D^* \cdot U \cdot |U| + C_M^* \cdot \dot{U} \tag{7}$$

where the coefficients C_D^* and C_M^* are assumed constants which take care of all variables like geometry of armour units, Reynold's number, surface roughness etc.

According to linear wave theory we have

$$S_{UU}(\omega) = \omega^2 \frac{\cos h\ k(z+d)}{\sin h\ k\,d}\ S_{\eta\eta}(\omega) \tag{8}$$

$$S_{\dot{U}\dot{U}}(\omega) = \omega^2 \cdot S_{UU}(\omega) \tag{9}$$

Eg. 7 is linearized as follows

$$\sigma = C_D^* \cdot U \cdot \sqrt{Var\ U} + C_M^* \cdot \dot{U} \tag{10}$$

where $Var\,U = \int S_{UU}\,(\omega)\,d\,a$.

C_D^* and C_M^* can be estimated such that there is minimum deviation between the actually recorded signal $\sigma^{recorded}(t)$ and σ from eq. 7.

With given C_D^* and C_M^* we can calculate

$$S_{\sigma\sigma}(\omega) = \frac{1}{2\pi} \int_{-\infty}^{\infty} R(\tau)\, e^{-i\omega\tau}\ d\tau$$

where $R(\tau)$ is the autocorrelation function

$$\frac{1}{T} \int_0^T \sigma(t)\ \sigma(t+\tau)\, dt = E\,[\sigma(t)\ \ \sigma(t+\tau)]$$

With known $S_{\sigma\sigma}(\omega)$ the transfer function can be calculated as follows:

$$|H(\omega)|^2 = \frac{S_{\sigma\sigma}(\omega)}{S_{\eta\eta}(\omega)} \tag{11}$$